Research Report

2008-26

Digital Charge Control of Boost Converter with Constant Power Machine Load

H. Xu*, X. Wen*, T. A. Lipo****

*Institute of Electrical Engineering
Chinese Academy of Sciences
Beijing, China

**University of Wisconsin-Madison
Madison, WI, USA

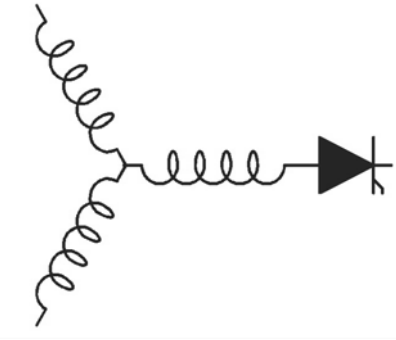

Wisconsin
Electric
Machines &
Power
Electronics
Consortium

University of Wisconsin-Madison
College of Engineering
Wisconsin Power Electronics Research Center
2559D Engineering Hall
1415 Engineering Drive
Madison WI 53706-1691

Digital Charge Control of Boost Converter with Constant Power Machine Load

Haiping Xu[1,2] , Xuhui Wen[1], Thomas. A. Lipo[2]
[1]Institute of Electrical Engineering, Chinese Academy of Sciences, Beijing, China
[2]University of Wisconsin-Madison, WI 53706, USA
Email: hpxu@mail.iee.ac.cn

Abstract—**This paper proposes the digital charge control method to boost converter operating with a type of nonlinear load, the constant power load. The constant power load is modeled theoretically, and model parameters are given in detail. Transfer functions of the boost converter with constant power load are deduced, and a small-signal model of the charge controlled current inner loop is presented. The Digital Charge Control method (DCC) is implemented with TMS320LF2407. A novel Digital Forecasting Charge Control method (DFCC) is proposed to eliminate the defect of duty-cycle jumping. The system stability and dynamic performance are analyzed thoroughly. Experimental results confirm that DFCC boost converter operating with the constant power machine load can follow the reference stably and rapidly.**

Keywords: charge control; DC-DC converter

I. INTRODUCTION

In recent years, PWM controlled DC-DC converters have been widely used, and control methods of DC-DC converters have been developed too. The voltage mode control, the current mode control [1]are used on various converters. Usually they are studied with resistor loads, and in most cases resistors are accurate enough approximations of the load characteristics. However, DC-DC converters have also been used as power sources of motors, such as in electric vehicles. Motors are dynamic loads, which may operate on different states as constant current or constant power[2]. On these states the behaviors of loads are all nonlinear, rather than linear which the resistor is. Nonlinear load cannot be approximated as resistors simply, and traditional control methods are not enough to maintain the converter stable output on these conditions.

Charge control is a new control method for DC-DC converters [3] [4]. Using this method, the perturbations of the load and the line changes can be eliminated rapidly, theoretically in one switching cycle. Nowadays, charge control is based on analog circuits. As one knows, DSP controllers are more flexible than analog controllers. In this paper, a novel digital charge control is proposed to boost converter operating with a constant power load. The forecasting technique is applied in the control program to eliminate the defect of duty-cycle jumping, which may occur in the digital control method. A TI DSP TMS320LF2407 is used to compose the digital controller for a boost converter.

In section II, the constant power load is analyzed and transfer functions of the boost converter with a constant power load are deducted. In section Ⅲ, charge control is introduced and applied to the converter, and then a current closed loop is constructed. In section IV, the digital charge control principle is presented. In section V, the novel digital forecast charge control method DFCC is described. The system stability and dynamic performance are analyzed in section VI. The experimental results are compared in section VII. Conclusions are given in section VIII.

II. MODELING OF BOOST CONVERTER WITH CONSTANT POWER LOAD

The load characteristic of a constant power load (CPL) is shown in Fig. 1. Defining v_O as the converter's output voltage and i_O as the output current.

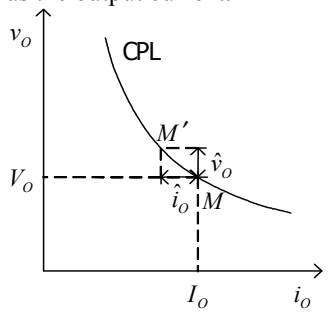

Fig. 1. Voltage and current characteristics of constant power load.

Firstly, assume that the load is operating on a point of the CPL (constant power load) curve, $M(V_O, I_O)$, and M is a steady operating point. The steady impedance is a resistance

$$R_{DC} = V_O / I_O . \tag{1}$$

Secondly, assume that there are small perturbations on the output voltage and output current, $v_O = V_O + \hat{v}_O$, $i_O = I_O + \hat{i}_O$. From Fig. 1 one knows that the dynamic impedance of the constant power load is

$$Z_{AC} = \hat{v}_O / \hat{i}_O \approx \left(dv_O / di_O\right)\Big|_{(V_O, I_O)} . \tag{2}$$

Assuming P is the input power of the load. $P = v_O i_O$. Taking the derivatives of the two sides of the equation,

$$d(P) = i_O \cdot dv_O + v_O \cdot di_O . \tag{3}$$

Because P is a constant, $d(P) = 0$, then

$$i_O \cdot dv_O + v_O \cdot di_O = 0 \tag{4}$$

$$dv_O / di_O = -v_O / i_O , \tag{5}$$

$$\left(dv_O / di_O\right)\Big|_{(V_O, I_O)} = -V_O / I_O . \tag{6}$$

From (1) (2), and (6), the dynamic impedance of the constant power load is a negative resistance.

$$Z_{AC} = -R_{AC} = -V_O / I_O . \quad (7)$$

Two parameters are necessary to model a constant power load. The first is the steady resistance R_{DC}. The second is the dynamic impedance Z_{AC}, which is a negative resistance, and the absolute value of Z_{AC} just equals to the steady resistance R_{DC}.

The steady state model and small-signal model of boost converter with continued inductance current are given in Fig. 2. The constant power load is replaced by R_{DC} and Z_{AC}.

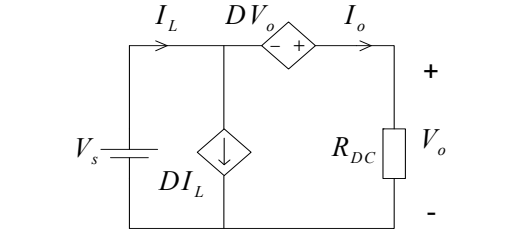

(a) Steady state model

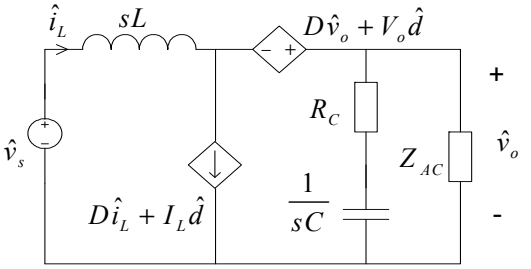

(b) Small-signal model

Fig. 2. Models of the boost converter with a constant power load.

From Fig. 2(a), one obtains the steady state equations

$$V_S - D'V_O = 0 , \quad (8)$$

$$I_L = DI_L + I_O . \quad (9)$$

Where V_S, V_O, I_L, I_O, D are the steady components of v_S, v_O, i_L, i_O, d respectively, and $D' = 1 - D$.

$$M = V_o / V_s = 1/D' , \quad (10)$$

$$I_O = I_L D' . \quad (11)$$

From Fig. 2(b), we get the small-signal equations

$$\hat{v}_s - \hat{i}_L \cdot sL - (1-D)\hat{v}_o + V_o\hat{d} = 0 , \quad (12)$$

$$\hat{i}_L = D\hat{i}_L + I_L\hat{d} + \hat{v}_o / \left(R_C + \frac{1}{sC} \right) + \hat{v}_o / Z_{AC} . \quad (13)$$

Where $\hat{v}_S$, $\hat{v}_O$, $\hat{i}_L$, $\hat{i}_O$, $\hat{d}$ are the perturbation components of v_S, v_O, i_L, i_O, d respectively. From (12), (13), we get the control to output voltage transfer function and the control to inductance current transfer function,

$$G_{vd} = \left. \frac{\hat{v}_o}{\hat{d}} \right|_{\hat{v}_s = 0} = \frac{V_S (sCR_C + 1)(1 - sL'/R_{DC})}{D'^2 (1 + s/Q\omega_0 + s^2/\omega_o^2)} , \quad (14)$$

$$G_{id} = \left. \frac{\hat{i}_L}{\hat{d}} \right|_{\hat{v}_s = 0} = \frac{sCV_o}{D'^2 (1 + s/Q\omega_0 + s^2/\omega_o^2)} . \quad (15)$$

$$L' = L / D'^2 , \quad (16)$$

$$\omega_0 = \sqrt{1/(L'C)} , \quad (17)$$

$$Q = Z_{AC} / \left[\omega_0 \left(Z_{AC} C R_c + L' \right) \right] . \quad (18)$$

The necessary condition to maintain the system's open-loop stable is $Z_{AC} CR + L' > 0$.

III. CHARGE CONTROL OF BOOST CONVERTER

Charge control is a particular type of nonlinear control technique. This technique achieves instantaneous dynamic control of the average value of the switched variable; theoretically it takes only one switching cycle to reach a new steady state. The principle of charge controlled boost converter with CPL is shown in Fig. 3.

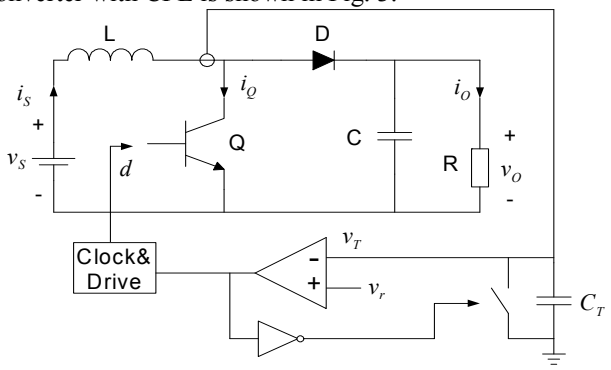

Fig. 3. The principle of charge control.

The constant switching period T_S is decided by the clock. At the beginning of each switching cycle, the active switch Q in the power stage is turned on. When the switch is on, the DC source v_S, the inductance L and the active switch Q compose a closed loop. The inductor current i_S equals to the switch current i_Q. The capacitor C_T is charged by i_Q through a current sensor as the switch Q is on. The voltage $v_T(t)$ rises from 0V. Supposing that the beginning time of a switching cycle is kT_S and the switch is keeping on to the time $kT_S + t_0$,

$$\int_{kT_S}^{kT_S + t_0} i_Q(t)dt = v_T(kT_S + t_0)C_T . \quad (19)$$

When the voltage $v_T(t)$ reaches the reference voltage v_r, the switch Q is turned off, and the switch across capacitor C_T is turned on to discharge C_T. C_T is totally discharged before the next switching cycle starts. In a switching cycle,

$$\int_{kT_S}^{kT_S + dT_S} i_Q(t)dt = v_r C_T = I_Q T_S . \quad (20)$$

In (20), d is the duty-cycle and I_Q is the average current of the switch for the whole switching cycle. The reference voltage v_r determines the charge passing through the switch Q in one cycle. The charge is in proportion to I_Q, as the switching period T_S is constant. Then v_r determined I_Q.

The small-signal model of charge controlled boost converter with CPL is shown in Fig. 4. F_m is the PWM modulator gain, and R_j , $H_e(s)$ represent the inductor current feedback. R_j is the equivalent current gain and $H_e(s)$ represents the sampled-and-hold effect in the current loop. We use K_r to represent the effect of the perturbation of output voltage on the duty- cycle.

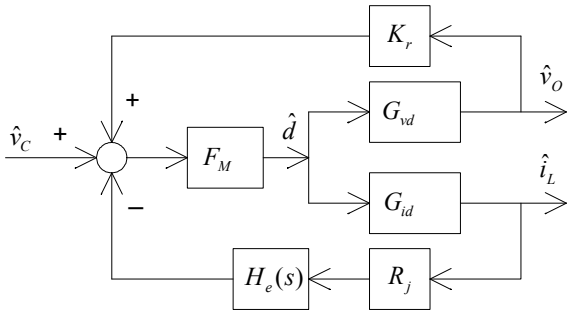

Fig. 4. Small-signal model of Charge controlled boost converter.

Attention should be paid to the fact that K_r is not a real feedback, but an equivalent feedback made by the inductor current feedback loop. In this model

$$K_r = R_j D'^2 T_S / (2L), \tag{21}$$

$$F_m = C_T / (I_{LP} T_S), \tag{22}$$

$$R_j = I_{LP} L / (C_T V_S). \tag{23}$$

I_{LP} is the peak inductor current and T_S is the switching cycle. A simple polynomial approximation for $H_e(s)$ is

$$H_e(s) = 1 + s/(\omega_n Q_n) + s^2/(\omega_n^2), \tag{24}$$

$$\omega_n = \pi / T_S, \tag{25}$$

$$Q_n = -2/\pi. \tag{26}$$

From Fig. 4, one obtains the input to output transfer function of the boost converter with a current loop

$$G_{oc} = \frac{\hat{v}_O}{\hat{v}_C} = \frac{F_M G_{vd}}{1 + R_j H_e(s) F_M G_{id} - K_r F_M G_{vd}}. \tag{27}$$

Applying (14), (15), and (21)-(24) to (27), and using some approximations, one get

$$G_{oc} \approx K \left(\frac{1 + sCR_c}{1 + s/\omega_{pL}} \right) \frac{(1 - sL'/R_{DC})}{1 + s/\omega_H Q_H + s^2/\omega_H^2}, \tag{28}$$

$$K = 2L'/(R_j T_S), \tag{29}$$

$$\omega_{pL} = T_S D'/(2L'C), \tag{30}$$

$$\omega_H = \pi / T_S, \tag{31}$$

$$Q_H = 1/[\pi (D' - 0.5)]. \tag{32}$$

G_{oc} is the transfer function of the boost converter with the one-cycle controlled current loop, which has two zeros and three poles.

IV DIGITAL CHARGE CONTROL PRICIPLE

To obtain the Digital Charge Control (DCC), a switching cycle must be divided into equal time slices. Supposing that the time of one slice is T_o, we have the switch current graph in Fig. 5. The switch current is sampled every T_o through the sensor from the beginning time of a switching cycle kT_S.

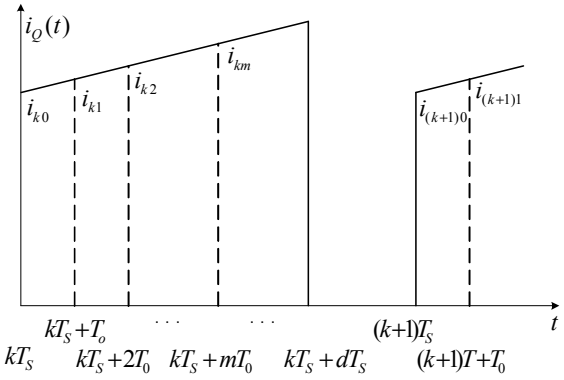

Figure5. Switch current of a boost converter.

Supposing that at time kT_S , $kT_S + T_0$, $kT_S + 2T_0$ ⋯ $kT_S + m\tau$ ⋯, the corresponding switch currents are i_{k0} , i_{k1} , i_{k2} ⋯ i_{km} ⋯. Sampling switch currents can be used to develop the current integral. At time $kT_S + T_0$, $kT_S + 2T_0$, $kT_S + 3T_0$, $kT_S + m\tau$, the integrals of currents are

$$Q_1 = \frac{1}{2}(i_{k0} + i_{k1}) T_0, \tag{33}$$

$$\begin{aligned} Q_2 &= \frac{1}{2}(i_{k0} + i_{k1}) T_0 + \frac{1}{2}(i_{k1} + i_{k2}) T_0 \\ &= Q_1 + \frac{1}{2}(i_{k1} + i_{k2}) T_0, \end{aligned} \tag{34}$$

$$\begin{aligned} Q_3 &= \frac{1}{2}(i_{k0} + i_{k1}) \tau + \frac{1}{2}(i_{k1} + i_{k2}) T_0 + \frac{1}{2}(i_{k2} + i_{k3}) T_0 \\ &= Q_2 + \frac{1}{2}(i_{k2} + i_{k3}) T_0, \end{aligned} \tag{35}$$

$$\begin{aligned} Q_m &= \frac{1}{2}(i_{k0} + i_{k1}) T_0 + \frac{1}{2}(i_{k1} + i_{k2}) T_0 + \cdots \\ &+ \frac{1}{2}(i_{k(m-1)} + i_{km}) T_0 = Q_{m-1} + \frac{1}{2}(i_{k(m-1)} + i_{km}) T_0. \end{aligned} \tag{36}$$

The integral is done after every sampling, and the integral is compared to the reference $v_r C_T$. If the integral is less than the reference, the active switch continues being on. If the integral is larger than or equals to the reference, the active switch is turned off immediately. Supposing that the switch is turned off after nT_0 from the beginning of a switching cycle nT_0 equals to dT_S approximately. A DSP control program can be obtained directly, but the adjacent duty-cycles may vary obviously when the output voltage is regulated, because it is the integral multiple of the time slice. The obvious duty-cycle variety is called duty-cycle jumping here. Duty-cycle jumping has disadvantageous effect on the stability of the system.

V. DIGITAL FORECAST CHARGE CONTROL METHOD

A novel Digital Forecast Charge Control method (DFCC) has been designed to eliminate the duty-cycle jumping. The DSP used here is TMS320LF2407. The control program

contains three parts. The first part is the main program, in which the DSP system is initialized. The second part is the General-Purpose Timer 1(GP T1) period interrupt service program, shown in Fig.6. The last part is the GP T2 period interrupt service program, shown in Fig.7.

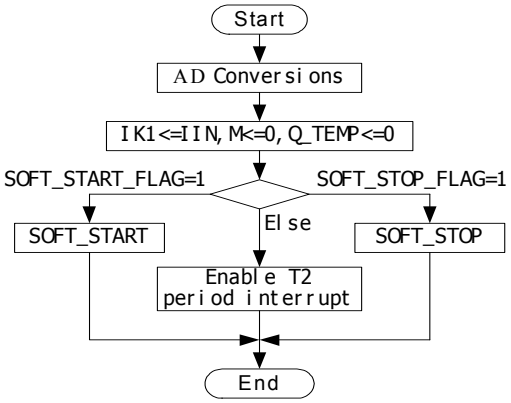

Figure6. GP T1 period interrupt service program flow chart.

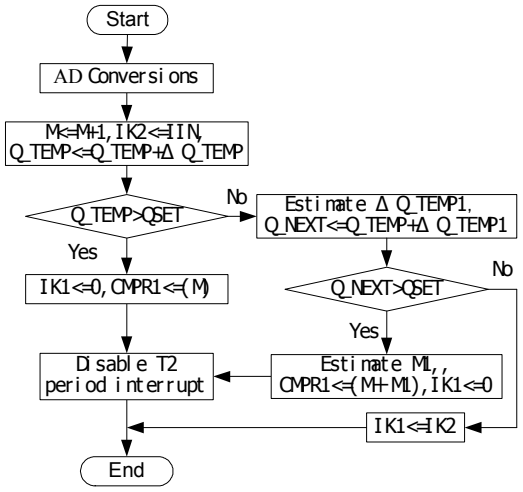

Figure7. GP T2 period interrupt service program flow chart of the DFCC method.

The period of the T1 interrupt is the switching period T_S, and the period of T2 interrupt is the time slice T_o.

In the program, the variable Q_{SET} represents the reference $v_r C_T$, Q_TEMP is the current integral, ΔQ_TEMP is the current integral of one time slice, M is the number of time slices passing by, IIN is the sampling current, $IK2$ is the sampling current this time slice, and $IK1$ is the sampling current last time slice. ΔQ_TEMP1 is the estimated current integral of the coming time slice, $M1$ is a fraction of the coming time slice. When the current integral Q_TEMP is less than the reference Q_{SET}, we estimate the current integral Q_NEXT at the end of the coming time slice, and then compare Q_NEXT and Q_{SET}. IfQ_NEXT is larger than Q_{SET}, the active switch should be turn off in the coming time slice.

The key point of DFCC method is how to estimate the turn-off time of the switches. It is a problem of solving the nonlinear equations. The switch current slice of switching period K is shown in Fig. 8.

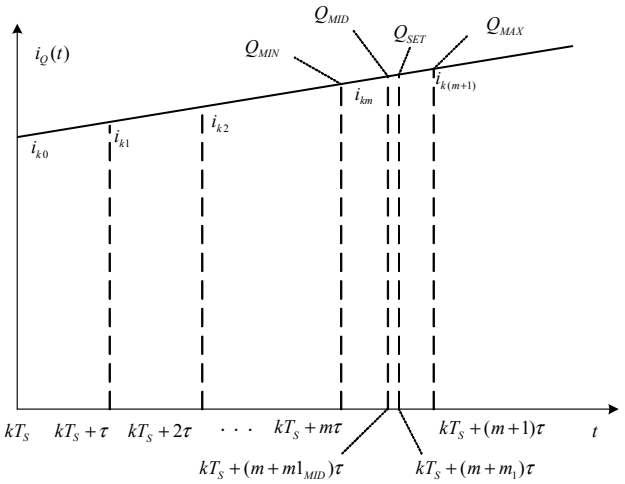

Figure 8. The forecast method of charge control.

Supposing the turn-off time of the switch corresponding to Q_{SET} is $(m+m_1)\tau$, $0<m_1<1$, it is mean that the turn-off time of switch is between the time $kT_S+m\tau$ and $kT_S+(m+1)\tau$. The problem is how to solve the m_1.

Assuming: $m1_{MIN}=0$, $m1_{MAX}=1$,

$m1_{MID}=(m1_{MIN}+m1_{MAX})/2$.

At time $kT_S+m\tau$, the Q_{MIN} is calculated by switch current integral. Substituting the switch current $i_{k(m+1)}$ at time $kT_S+(m+1)\tau$ with the i_{km} at time $kT_S+m\tau$, the charge value of next slice time, Q_{MAX}, is forecasted. The charge value Q_{MID} at time $kT_S+(m+\mathrm{m1_{MID}})\tau$ is calculated by average method.

Comparing Q_{MID} with Q_{SET}, if Q_{SET} is large than Q_{MID}, the new value of $m1_{MIN}$ and $m1_{MID}$ are re-calculate by the following equations,

$$m1_{MIN} = m1_{MID} \quad (37)$$

$$m1_{MID} = (m1_{MIN}+m1_{MAX})/2 \quad (38)$$

If Q_{SET} is less than Q_{MID}, the new value of $m1_{MAX}$ and $m1_{MID}$ are re-calculate by the following equations,

$$m1_{MAX} = m1_{MID} \quad (39)$$

$$m1_{MID} = (m1_{MIN}+m1_{MAX})/2 \quad (40)$$

Then the new Q_{MID} at time $kT_S+(m+\mathrm{m1_{MID}})\tau$ is calculated. The process of above is performed again and again until the following condition is set,

$$|Q_{SET}-Q_{MID}| \le Q_{LIM}$$

$\mathrm{Q_{LIM}}$ is the small set value of ending circulation.

At this point, $m_1 = m1_{MID}$

The program for forecasting M1 is showed in Fig. 9.

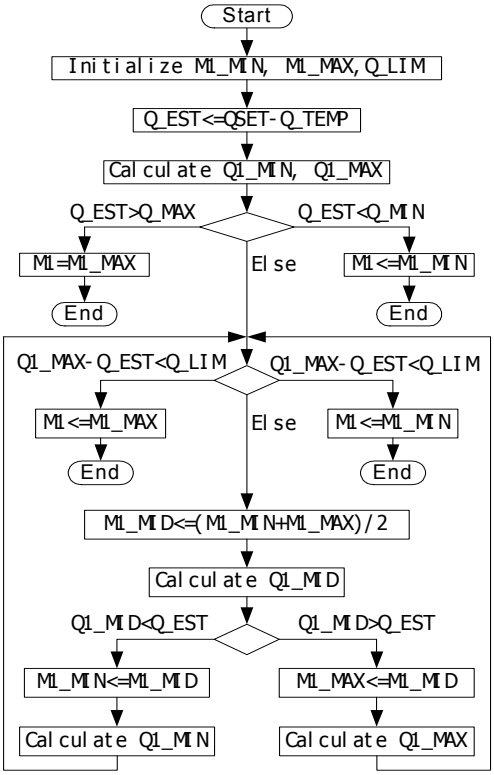

Figure 9. Program for forecasting M1.

The main part of the duty-cycle comes from current integral, so the DFCC method maintains the advantage of fast dynamic response in charge control. The duty-cycle does not jump, because it is not the integral multiple of the time slice any more. Meanwhile, in the DCC method, if the switch period is equal to sampling period multiplying n, the accuracy of output voltage is $\frac{V_S}{n}$. In the DFCC method, if Q_{LIM} is equal to the charge value of one sampling period multiplying $\frac{1}{l}$, the accuracy of output voltage will be $\frac{V_S}{nl}$. So, comparing the DFCC method with the DCC method, the accuracy of output voltage and adjustment ability of controller is increased many times.

VI System Stability and Dynamic Performance

The system stability and dynamic performance of DFCC control boost converter with constant power load is studied. The parameter of boost converter is as follow,

$V_S = 200V$, $V_O = 320V$, $L = 800\mu H$, $C = 2200\mu F$, $T_S = 200\mu s$, $P = 5000W$, $v_C = 2\text{V}$ $R_C = 0.02\Omega$,

The input to output transfer is,

$$G_{or} \approx \frac{(1+sCR_C)(1-sL_e/Z_{DC})}{\frac{R_j T_S}{2L_e}\left(1+\frac{2L_eC}{T_S D'}s\right)\left(1+T_S(D'-0.5)s+\frac{s^2}{\omega_H^2}\right)}$$

$$\approx \frac{(1+s\times 44\times 10^{-6})(1-s\times 100\times 10^{-6})}{7.16\times 10^{-3}\times\left(1+s\times 72.09\times 10^{-3}\right)\left(1+s\times 25\times 10^{-6}+s^2\times 4.05\times 10^{-9}\right)}$$

$$\approx \frac{139.67\times(1+s\times 44\times 10^{-6})(1-s\times 100\times 10^{-6})}{\left(1+s\times 72.09\times 10^{-3}\right)\left(1+s\times 25\times 10^{-6}+s^2\times 4.05\times 10^{-9}\right)}$$

The Nyquist Diagram is shown in Fig. 10a. Fig. 10b is the local diagram near point (-1,0). The system is stable.

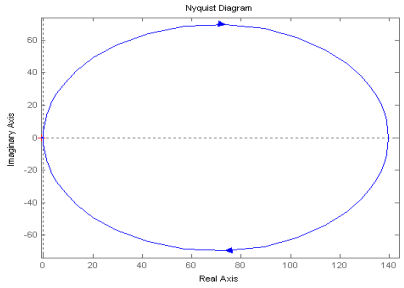

(a) The entire diagram

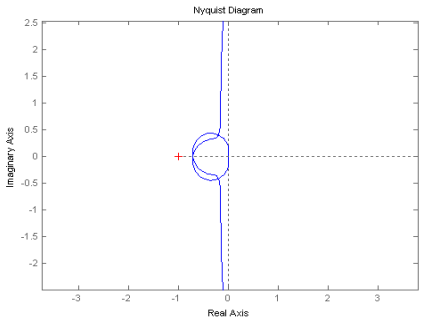

(b) The partial diagram near point (-1,0)

Fig. 10. Nyquist diagram for DFCC boost converter.

To maintain the output voltage constant or following the reference, a closed loop of voltage is necessary. With the inner current loop and the outer voltage loop, the boost converter becomes a system with two closed loops. The dynamic response of the system can be shown in Fig. 11, when there is an identify step change at reference $\hat{v}_r$, the response of output $\hat{v}_O$ can follow the change of the reference within 2 ms, and the characteristic of the output voltage has been improved enormously.

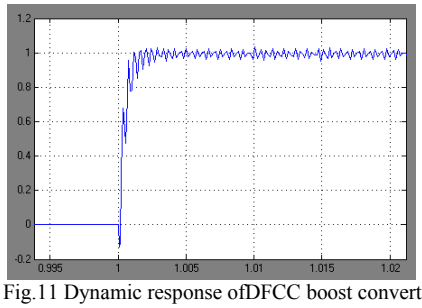

Fig.11 Dynamic response ofDFCC boost converter.

VII EXPERIMENT RESULTS

Based on the analysis above, using DSP-320F2407 as main controller, a prototype of DFCC boost converter with constant Power load was constructed. The basic technical specification of the system is as follows: Pin=3838W, Pout=3528W, Vs =202V, V0 =336V, Iin=19.0A, Iout=10.5A.

PWM Switching signals of DCC method and DFCC method can be seen in Fig. 12. The figure confirms that the duty-cycle jumping will arise using the DCC method, and the DFCC method can eliminate this defect.

Figures.13 are the waveforms of the DFCC boost Converter with constant power load. Fig 13a are voltage ripple of input and output before start-up. The ripple of input voltage is 1.62Vrms. Fig 13b are voltage ripple of input and output after start-up. The ripple of input voltage is the same as fig 13a. The ripple coefficient of input voltage is 0.80%. The ripple of output voltage is decrease evidently to 0.95Vrms, and the ripple coefficient of output voltage is only 0.28%. Fig 13c is the waveforms of inductor current and PWM signal to switch. Fig 13d is the waveforms of dynamic step response of output voltage, in which the dynamic response time is less than 50ms. The experimental results demonstrate the DFCC boost converter has the favorable output performance.

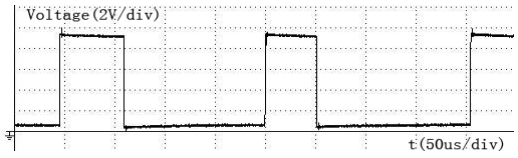

(a) Switching signal in the DCC controller

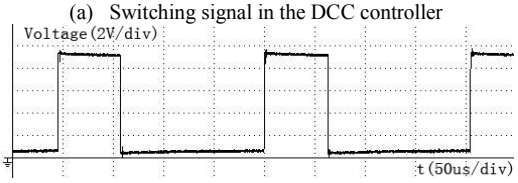

(b). Switching signal in the DFCC controller

Figure 12. Comparison of switching signals

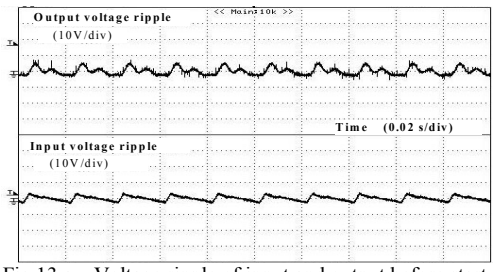

Fig 13 a Voltage ripple of input and output before start-up

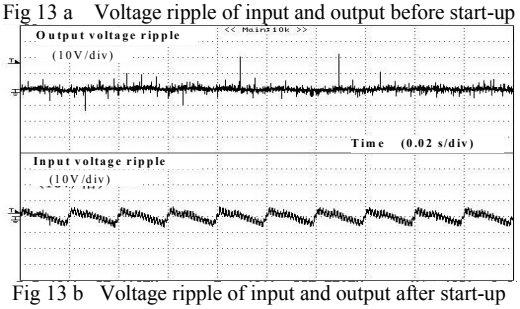

Fig 13 b Voltage ripple of input and output after start-up

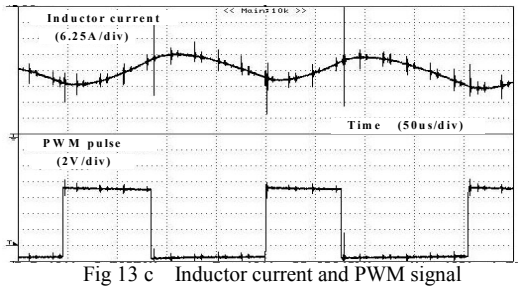

Fig 13 c Inductor current and PWM signal

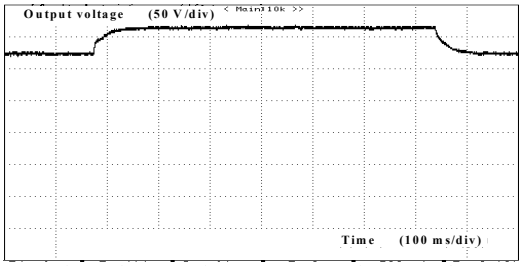

Fig 13 d Dynamic step response of output voltage.

VIII. CONCLUSIONS

A steady state resistor and dynamic impedance are used to model the constant power load. The steady resistor is used to determine the steady operating point and the dynamic impendence is used in the small-signal model to study the dynamic characteristics. Charge control is a nonlinear control method, which can eliminate perturbations of the load and line changes rapidly. The digital charge control DCC is presented and analyzed based on the time slice division. but it has the defect of the duty-cycle jumping. The improved digital forecast charge control method DFCC can eliminate the duty-cycle jumping. Steady operating point, small-signal models, and Nyquist diagrams are used to analyze the stability and dynamic performance of the system.

Experimental and simulation results confirm that DFCC boost converter operating with the constant power load have the favorable dynamic performance, follow the reference stably and rapidly. The DFCC method can be extensively used in DC-DC converter with linear or nonlinear load.

REFERENCES

[1] Byungcho Choi, “Step load response of a current-mode-controlled DC-to-DC converter,” IEEE Trans. Aerosp. Electron. Syst., vol. 33, no. 4, Oct. 1997

[2] V. Grigore, J. Hatonen, J. Kyyra, and T. Suntio, “Dynamics of a Buck Converter with a Constant Power Load,” in Proc. IEEE Power Electronics Specialists’ Conf., vol. 1, pp. 72–78, 1998

[3] Wei Tang, F. C. Lee, R. B. Ridley, and Isaac Cohen, “Charge control: modeling, analysis, and design,” IEEE Trans. Power Electron., vol. 8, no. 4, Oct. 1993.

[4] Shi wenqing, Xu Haiping, Wen Xuhui, Wen Wei, “One-Cycle Controlled DC-DC Converters Operating with Nonlinear Power Load,” ICEMS., vol. Ⅱ, pp.1361~1365, Sept.2005